

Tungsten Disilicide (WSi_2): Synthesis, Characterization, and Prediction of New Crystal Structures

Jelena Luković,^{*,[a,b]} Dejan Zagorac,^{*,[a,b]} J. Christian Schön,^{*,[c]} Jelena Zagorac,^[a,b] Dragana Jordanov,^[a,b] Tatjana Volkov-Husović,^[d] and Branko Matović^[a,b]

Dedicated to Professor Thomas Schleid on the Occasion of his 60th Birthday

Abstract. Transition metal silicides have attracted great attention due to their potential applications in microelectronics, ceramics, and the aerospace industry. In this study, experimental and theoretical investigations of tungsten based silicides were performed. Tungsten disilicide (WSi_2) was synthesized by simple thermal treatment at 1350 °C for 4 h in an argon atmosphere. These optimal synthesis conditions were obtained by variation of temperatures and times of heating, and the

structure of the final synthesized compound was determined by XRPD analysis. In addition, new modifications for WSi_2 were proposed and investigated using first-principles calculations within density-functional theory (DFT). Both LDA and PBE calculations show excellent agreement with experimental observations and previous calculations for the existing modifications, where available.

1 Introduction

With the extremely fast growth of technology and industry in the last decades has come the constant need for materials with improved characteristics and better performance under extreme conditions. In the metallurgical and the chemical industry, and in advanced technologies, the materials used are frequently subjected to extreme conditions such as exposure to chemical and mechanical stresses, and operation at high temperatures.^[1,2] Tungsten based silicides, and in particular tungsten disilicide (WSi_2) with melting point above 2160 °C and pentatungsten trisilicide (W_5Si_3) with melting point above 2320 °C, respectively, appear suitable for operation in extreme conditions. In addition, WSi_2 has low electrical resistivity and good thermal stability, and it has been investigated as a protective coating on W-based alloys because of its excellent oxidation resistance.^[3–6] Another area of application are integrated circuits, where one goal is to replace polycrystalline silicon with materials with lower resistivity. Thus, refractory metal silicides have been introduced as possible candidates for this

application. Furthermore, W_5Si_3 coatings exhibit great abrasive and adhesive wear resistance.^[7] Tungsten based silicides are also used as additives, where WSi_2 and W_5Si_3 are included as suitable materials for mixing with e.g. WC, in order to overcome the problem of oxidation in extreme conditions, for applications in the metal and cutting tools industries.^[8,9]

In the past, a variety of synthesis methods have been used for the production of tungsten silicide. Several different approaches can be distinguished: deposition methods for formation of thin films (by sputtering),^[10] by ion beam bombardment,^[11] or ion beam mixing with rapid thermal annealing,^[12,13] by low-pressure chemical vapor deposition,^[14–16] and by cold wall deposition (employing CVD).^[15,17] Kim et al. have discussed the transformation of WSi_2 into W_5Si_3 at elevated temperatures, which has been experimentally confirmed by Kharatyan et al.^[4,18]

The experimentally known modification of tungsten disilicide (WSi_2) crystallizes in the tetragonal space group $I4/mmm$ (no. 139). Furthermore, the equilibrium WSi_2 tetragonal modification is characterized as the MoSi_2 structure type (Strukturbericht designation C11_b , and Pearson symbol $tI6$).^[19–21] The MoSi_2 crystal structure is characteristic of the sequential stacking of the W and Si atomic layers along the c axis, with ten-fold coordination of tungsten by Si atoms (CN = 10, see Figure 1a). Another experimentally observed structure of WSi_2 at low temperatures and/or in thin films shows hexagonal symmetry with space group $P6_222$ (no. 180). In the literature, the hexagonal modification of tungsten disilicide has been defined as metastable with CrSi_2 type of structure (Strukturbericht designation C40 , and Pearson symbol $hP9$).^[22–24] The hexagonal WSi_2 modification keeps the ten-fold coordination of tungsten by Si atoms, but changes the coordination polyhedron (see Figure 1b).

* Dr. J. Luković
E-Mail: jelenal@vinca.rs;

* Dr. D. Zagorac
E-Mail: dzagorac@vin.bg.ac.rs;

* Prof. Dr. J. C. Schön
E-Mail: C.Schoen@fkf.mpg.de

[a] Institute of Nuclear Sciences Vinca
Materials Science Laboratory
University of Belgrade
Belgrade, Serbia

[b] Center for the synthesis, processing and characterization of materials for use in extreme conditions
Belgrade, Serbia

[c] Max Planck Institute for Solid State Research
70569 Stuttgart, Germany

[d] Faculty of Technology and Metallurgy
Department for Metallurgical Engineering
University of Belgrade
Belgrade, Serbia

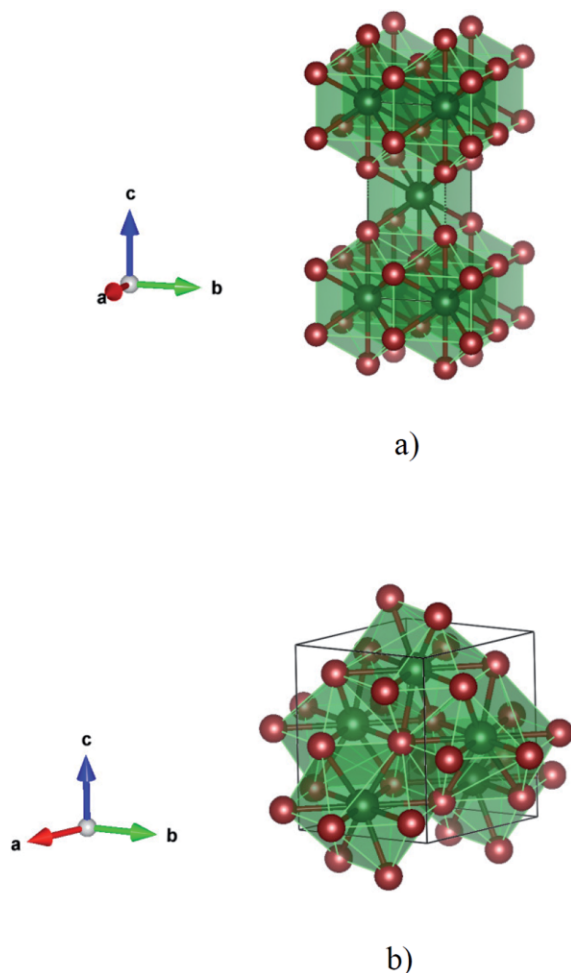


Figure 1. Visualization of the experimentally known WSi_2 structures (using the VESTA program): (a) equilibrium WSi_2 modification in the tetragonal MoSi_2 structure type; (b) metastable WSi_2 modification with hexagonal CrSi_2 structure type. Dark brown balls correspond to Si atoms, light green balls correspond to W atoms, respectively.

However, it seems that there are still many open questions regarding the structural behavior of WSi_2 , such as its dependence on grain size, composition, surface morphology, time of annealing, where even the conductivity can be dependent on the annealing temperature.^[22–25] Furthermore, since W and Si react to form WSi_2 at 1250 °C but form W_5Si_3 already at 1300–1400 °C, it is rather difficult to synthesize the pure silicide phases, without additional impurity phases, in large amounts.^[4,18] We hope that this study, which focuses on structural properties of WSi_2 , and combines experimental and theoretical investigations, will give some answers and provide a starting point for further research into new modifications of tungsten silicides and their respective properties.

2 Experimental Section

2.1 Experimental Methods

2.1.1 Preparation of Tungsten Silicide Powder

For this study, commercial tungsten powder (Koch-Light Laboratories, LTD, purity 99.9%) of average grain size of 1 μm according to manu-

facturer specification, and commercial silicon powder were used as starting materials for the synthesis of tungsten silicide powders. They were homogenized in acetone for 24 h. Starting powders were used in the stoichiometric ratio, while the ball-to-powder ratio was 5:1. After homogenization and air drying, acetone evaporated. The prepared mixture was thermally treated at different temperatures ranging from 1250 to 1400 °C, with an increment of 50 °C. The heating rate was 10 $\text{K}\cdot\text{min}^{-1}$. The mixture was placed in a tube furnace, and the heat treatment was conducted in an argon flow for 4 h. After the treatment, the furnace was cooled to room temperature.

2.1.2 XRPD Analysis

Tungsten silicide powders were characterized by X-ray powder diffraction (XRPD) with a Rigaku Ultima IV diffractometer using $\text{Cu-K}\alpha$ radiation and a Ni filter. In order to derive the relevant structural parameters, experimental data for Rietveld refinement were taken at a speed of 2° per min in a range of diffraction angles 2θ of 5–80°, with an angular resolution of 0.02°. Structural analysis was carried out using Rietveld refinement and the program FullProf.^[26]

2.2 Computational Methods

The full geometry optimizations for each proposed modification was performed using the CRYSTAL14 code,^[27,28] which is based on a Linear Combination of Atomic Orbitals (LCAO). For the ab initio calculations, a $[5s4p1d]$ all-electron basis set (AEBS) was used for silicon, labeled Si_86-311G**_pascal_2005.^[29] For tungsten, we have used the $[4s4p2d]$ pseudopotential, labeled ECP60MWB.^[30] The local optimizations employed analytical gradients with respect to the atom positions,^[31] and the cell parameters,^[32] and a local optimization routine.^[33] These local optimizations were performed using Density Functional Theory (DFT). It is reasonable to choose at least two different ab initio methods, in order to gain better insight in the quantitative validity of the results.^[34–37] Thus we have used the Local Density Approximation (LDA) with Perdew-Zunger (PZ) correlation functionals,^[38] and the Generalized Gradient Approximation (GGA) with the Perdew-Burke-Ernzerhof (PBE) functional, for comparison.^[39] The $E(V)$ curves were calculated using constant volume optimization on a point-by-point basis, by relaxing the crystalline structure at a sequence of fixed cell volume values, where the shape of the cell was allowed to be varied. Reference geometry to classify integrals was used with the keyword FIXINDEX in order to obtain a smooth curve, finally subjected to polynomial curve fitting.^[27,28]

Since it is possible, in principle, that additional symmetries appear during the local optimization, the symmetry of the optimized structures was analyzed with the algorithms SFND (“Symmetry FiNDer”^[40]) and RGS (“Raum Gruppen Sucher” = space group seeker^[41]), as implemented in the program KPLOT.^[42] The CMPZ algorithm^[43] implemented in the KPLOT program was used to compare the various crystal structures. The structures investigated were visualized using KPLOT^[42] and the VESTA^[44] software.

3 Results and Discussion

3.1 XRPD Analysis of Tungsten Silicides

As mentioned earlier, tungsten and silicon react to form tungsten disilicide (WSi_2) at 1250 °C, and pentatungsten trisilicide (W_5Si_3) at higher temperatures (1300 to 1400 °C), respectively. The temperature of 1400 °C is sufficiently high for the conversion of the starting materials to tungsten based

silicides without any remains of unreacted tungsten and silicon, but impurities like WC are present in the material, probably due to the presence of carbon content in the furnace, leading to a reaction with tungsten to form WC. Heating for 4 h at 1350 °C leads to a complete conversion of those elementary powders to WSi_2 and W_5Si_3 . This is clearly confirmed in Figure 2, which shows the XRPD patterns of the sample after heating at 1350 °C for 4 h in an argon flow.

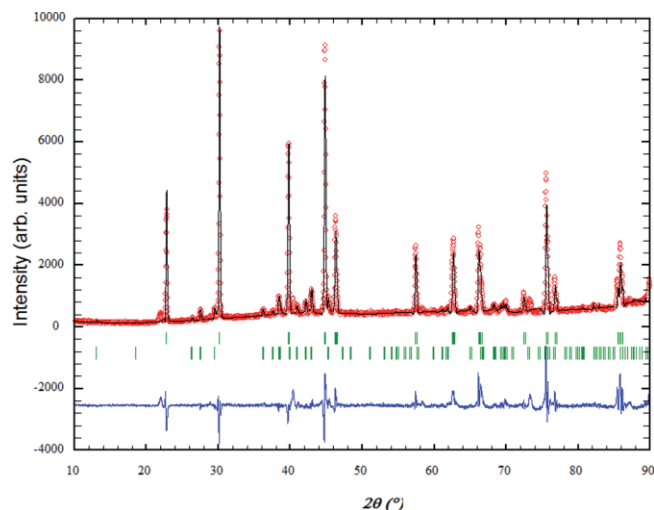


Figure 2. Rietveld diagram of WSi_2 and W_5Si_3 powders obtained after heating at 1350 °C for 4 h in an argon atmosphere. Blue line denotes difference between experimental (red diamonds) and theoretical (black line) profile, while the Bragg positions are indicated by vertical green slashes.

The X-ray analysis showed a two-phase composition for the investigated sample, where the WSi_2 phase is dominant (ca. 85 mass %) compared to W_5Si_3 . This suggests that further fine-tuning of the synthesis process should allow the production of nearly phase pure WSi_2 . The results of the Rietveld refinement are presented in Table 1.

Table 1. The parameters of the unit cells for the experimental phases obtained by Rietveld refinement.

	WSi_2	W_5Si_3
Space group (no.)	$I4/mmm$ (no. 139)	$I4/mcm$ (no. 140)
Unit cell parameters		
a / Å	3.2083(1)	9.5917(3)
b / Å	3.2083(1)	9.5917(3)
c / Å	7.8216(4)	4.9690(2)
α / °	90	90
β / °	90	90
γ / °	90	90
Volume V / Å ³	80.5075	457.1598
Atomic positions		
(x,y,z)		
W1	0 0 0	0 0.5 0.25
W2		0.075(1) 0.222(1) 0
Si1	0 0 0.322(1)	0 0 0.25
Si2		0.168(6) 0.668(6) 0

3.2 Modeling of WSi_2 on *ab initio* Level

Predicting, which crystalline modifications can exist in a chemical system or even, which unknown chemical system can

be synthesized, requires a global exploration of its energy landscape,^[45–47] in principle. The most common exploration methods have been described in detail elsewhere.^[48] However, if the interactions between the atoms cannot easily and robustly be described by simple empirical potentials (thus requiring the use of computationally expensive *ab initio* energy calculations) – as is the case for the W/Si system –, then a useful first step is to employ data mining based searches^[49–54] to gain an overview over the richness of the energy landscape. Thus, in this study, we have performed such searches starting from the ICSD database,^[55] where we have focused on related silicide systems, as well as related binary compounds. Besides the experimentally observed tetragonal MoSi_2 and hexagonal CrSi_2 modifications of WSi_2 , we have investigated several additional promising modifications of tungsten disilicides.

First, we note that since transition metal silicide based refractory composite alloys have great potential for applications as, for example, the next generation of aerospace materials, there are four crystal structures of known refractory disilicides that are worthwhile targets of investigation in the W-Si system: the CrSi_2 (C40) type, the MoSi_2 (C11b) type, the TiSi_2 (C54) type, and the ZrSi_2 (C49) type.^[56] Thus, we have investigated the related structures in WSi_2 on *ab initio* level, starting with the TiSi_2 structure type, which possesses orthorhombic symmetry with space group $FdddZ$ (no. 70) (Strukturbericht designation C54, and Pearson symbol $oF24$). This modification can be a good structure candidate, since the original TiSi_2 structure was preserved after the DFT optimization (confirmed using the CMPZ algorithm in KPLLOT), and it shows a ten-fold coordination of tungsten by Si atoms (CN = 10, see Figure 3a), similar to the experimentally observed structures. In addition there have been earlier theoretical suggestions^[57] of the TiSi_2 (C54) structure type for WSi_2 , in agreement with our DFT calculations.

Next, we have investigated the ZrSi_2 type of structure (Strukturbericht designation C49, and Pearson symbol $oC12$) in the W-Si system, another orthorhombic structure candidate. However, the original ZrSi_2 structure type was not preserved after the DFT optimization; instead we observe a novel ZrSi_2 -like type of structure in the WSi_2 system (cf. Figure 3b). Although the ZrSi_2 -like modification is showing space group $Cmcm$ (no. 63), like the original ZrSi_2 type, changes in crystal structure and coordination number are observed. The original ZrSi_2 type has 10 fold coordination of Zr by Si atoms, whereas the novel ZrSi_2 -like modification has 11 fold (2+4+5) coordination of W by Si atoms. In particular, the coordination polyhedron contains two silicon atoms sitting much closer to tungsten (ca. 1.7 Å) than the next four Si atoms, which are located about 2.5 Å away from the W atom (which is the average distance in other WSi_2 modifications). Finally, there are five distant Si atoms, which are about 3.7–3.8 Å away from the central tungsten atom.

Although it appears that WSi_2 can exist in a variety of seemingly complicated orthorhombic (the TiSi_2 and the ZrSi_2 -like), hexagonal (the CrSi_2 type), and tetragonal (the MoSi_2 type) modifications, they do in fact share a common structural building block that consists of nearly hexagonal WSi_2 layers. In

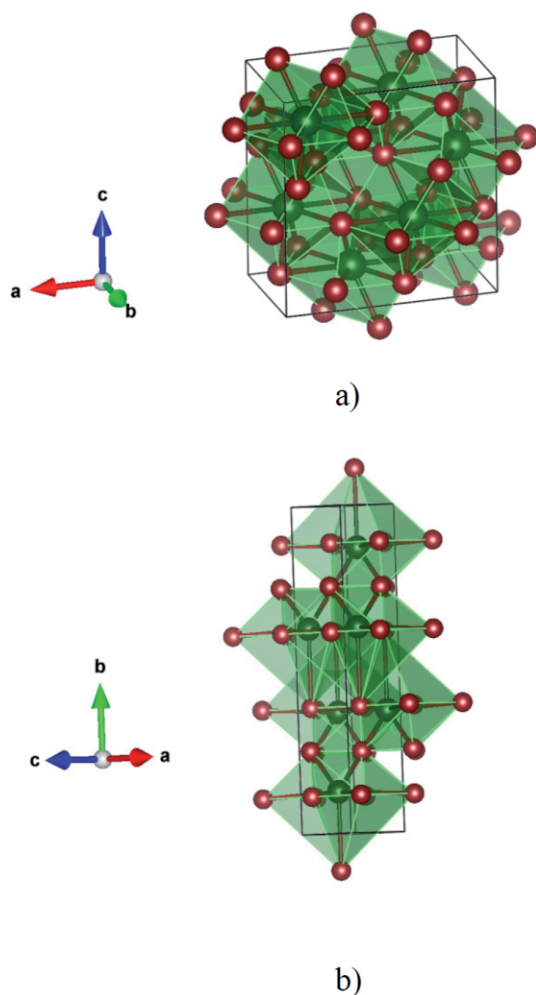


Figure 3. Visualization of two proposed modifications for the WSi_2 compound: (a) the TiSi_2 structure type; (b) the ZrSi_2 -like structure type. Dark brown balls correspond to Si atoms, light green balls correspond to W atoms, respectively.

particular, orthorhombic (the TiSi_2 type), hexagonal (the CrSi_2 type), and tetragonal (the MoSi_2 type) modifications can be generated by introducing simple variations in the stacking sequence of these nearly hexagonal WSi_2 layers.^[58–60] This structural systematic seems to be related to the d-band filling of the transition metal constituents of the structural prototypes, e.g. the group-IV disilicides form orthorhombic TiSi_2 or ZrSi_2 structures, that contain four-layer ($ABCD$) and two-layer (AB) stacking sequences, respectively. On the other hand, the group V compounds consistently adopt the three-layer (ABC) hexagonal CrSi_2 type structure, while the stable phases of the group VI materials include both the hexagonal CrSi_2 structure, and the two-layer (AB) tetragonal MoSi_2 type of structure. The transition from hexagonal to tetragonal symmetry among the isoelectronic group-VI compounds suggests a near degeneracy in the structural energies for these phases.^[58–60] This is supported by the fact that metastable hexagonal MoSi_2 and WSi_2 thin films can be formed using the ion-implantation technique and low annealing temperatures.^[22–24,60]

As an additional candidate suggested by our search through the ICSD, we have studied the SrSi_2 modification of the WSi_2 compound, which had not yet been investigated in the tungsten silicide system. The SrSi_2 structure type crystallizes in cubic symmetry with space group $P4_332$ (no. 212) (Pearson symbol $cP12$). After the local DFT optimization of the SrSi_2 -like modification of tungsten disilicide, the silicon atoms behave as three-covalent anions bonded to neighbors, whereas the W cations exhibit a sixfold coordination by silicon (CN = 6), with average distance of ca. 2.6 Å. In the original SrSi_2 compound, Sr is eightfold coordinated by silicon, with two longer axial bonds and six shorter pseudo-equatorial bonds. In the tungsten disilicide the Si-atoms of the longer axial bonds reside far away from the first coordination polyhedron (formed by the six nearest Si-neighbors of the tungsten atom, at distances of about 3.5 Å. This displacement effectively reduces the coordination to six; it is possibly due to a partially covalent character (see Figure 4a).^[61]

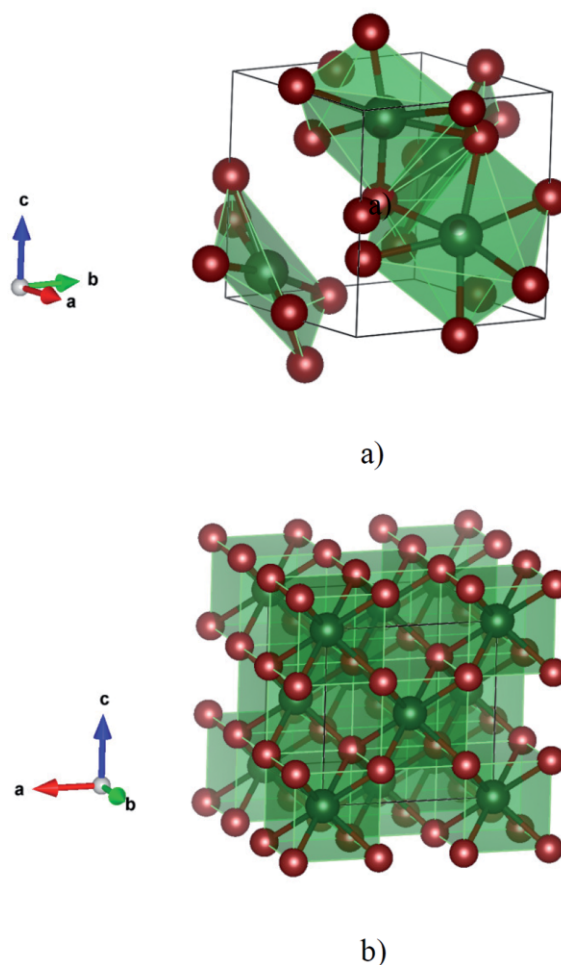


Figure 4. Visualization of two proposed structures in the WSi_2 system: (a) the SrSi_2 -like structure type; (b) the CaF_2 structure type. Dark brown balls correspond to Si atoms, light green balls correspond to W atoms, respectively.

Finally, we present another not-yet theoretically or experimentally observed structure in the W–Si system: the CaF_2 structure (Figure 4b). The CaF_2 structure type is another cubic

Table 2. Cell parameters and atom positions of the WSi_2 modifications observed in our experiments at 1350 °C and from earlier calculations in the literature, compared to the calculated/predicted WSi_2 modifications after local optimization on ab initio level using LDA and GGA-PBE functionals in this study. Note that the difference between the cell parameters determined by experiment (at ca. 1600 K) and by theory (at 0 K) is below 2%, which is very satisfactory considering the general limitations of DFT-calculations.

Modification and space group	Experiment ^{a)} / Theory ^{b,c)}	Cell parameters /Å and fractional coordinates	
		GGA-PBE ^{a)}	LDA ^{a)}
MoSi ₂ type – equilibrium <i>I4/mmm</i> (no. 139)	$a = 3.208, c = 7.821$ ^{a)} W (0 0 0) Si [0 0 0.322(1)]	$a = 3.249, c = 7.948$ W (0 0 0) Si (0 0 0.3346)	$a = 3.214, c = 7.887$ W (0 0 0) Si (0 0 0.3347)
CrSi ₂ type – LT phase <i>P6₃22</i> (no. 180)	$a = 4.614, c = 6.414$ ^{b)} W (0.5 0 0.5) Si (0.164 0.328 0.5)	$a = 4.656, c = 6.672$ W (0.5 0 0) Si (0.1639 0.3278 0)	$a = 4.607, c = 6.624$ W (–0.5 0 0) Si (0.1641 0.3282 0)
TiSi ₂ type – predicted <i>FdddZ</i> (no. 70)	$a = 7.838, b = 4.524, c = 8.959$ ^{c)}	$a = 8.060, b = 4.630, c = 8.976$ W (0.125 0.125 0.125) Si (–0.0377 –0.375 0.125)	$a = 7.964, b = 4.590, c = 8.906$ W (0.125 0.125 0.125) Si (–0.0383 –0.375 0.125)
ZrSi ₂ -like type – predicted <i>Cmcm</i> (no. 63)	$a = 3.180, b = 12.230, c = 4.151$ ^{c)}	$a = 3.486, b = 15.524, c = 3.391$ W (0.5 –0.1276 0.25) Si (0 0.0613 0.25) Si (0 –0.2478 0.25)	$a = 3.448, b = 15.283, c = 3.361$ W (0.5 –0.1266 0.25) Si (0 0.0610 0.25) Si (0 –0.2480 0.25)
SrSi ₂ -like type – predicted <i>P4₃32</i> (no. 212)	–	$a = 5.819$ W (0.125 0.125 0.125) Si (–0.2208 –0.2208 –0.2208)	$a = 5.755$ W (0.125 0.125 0.125) Si (–0.2202 –0.2202 –0.2202)
CaF ₂ type – predicted <i>Fm$\bar{3}$m</i> (no. 225)	–	$a = 5.927$ W (0 0 0) Si (0.25 –0.25 –0.25)	$a = 5.877$ W (0 0 0) Si (0.25 –0.25 –0.25)

a) This study. b) Reference^[22]. [c] Reference^[54].

structure candidate, showing space group $Fm\bar{3}m$ (no. 225). In the literature, it is known from the mineral fluorite (Pearson symbol $cF12$).^[62] Similar to the previous cubic candidate (SrSi₂), tungsten is eightfold coordinated by silicon atoms in the CaF₂ modification.

A complete list of the structure candidates calculated using DFT, with corresponding unit cell parameters and atomic positions, is presented in Table 2. Our DFT calculations are in very good agreement with our experimental results and previous experimental observations.^[8,9,19,20,22–24] Similarly, the calculations presented are in very good agreement with previous theoretical investigations where available.^[57,60,63] We note a slightly better agreement when using the LDA functional compared to the GGA-PBE results.

Regarding the kinetic stability of these predicted structures, we note that the local minimizations were performed without symmetry constraints and involved considerable displacements of the atoms in the case of the newly predicted structures, suggesting that the final structures are true local minima and not saddle points.

Finally, a total energy ranking is presented in Table 3, and $E(V)$ curves are shown in Figure 5. We observe that for the total energy ranking, the results of the calculations using the GGA functional are consistent and comparable with those for the LDA functional (Table 3). We note that the equilibrium WSi_2 modification is the lowest energy minimum regardless of DFT method used, which is in agreement with earlier experimental and theoretical data for a stable phase of WSi_2 at normal conditions. From the calculated $E(V)$ curves, the metastable CrSi₂ type has been observed as the closest calculated en-

ergy minimum to the equilibrium WSi_2 structure (see Table 3 and Figure 5). Again, our calculations are in a good agreement with previous experiments and calculations, where the CrSi₂ type modification had been found as a metastable structure, experimentally observed at low temperatures and/or in thin films.^[22–24]

Table 3. Calculated total energies of the WSi_2 modifications after local optimization on ab initio level, using LDA and GGA-PBE functionals. Energy per formula unit is given in hartree (E_h).

Modification	Total energy / E_h	
	GGA-PBE	LDA
MoSi ₂ type – equilibrium	–646.0386	–643.9394
CrSi ₂ type – LT phase	–646.0321	–643.9312
TiSi ₂ type – predicted	–646.0246	–643.9240
ZrSi ₂ -like type – predicted	–645.9949	–643.8929
CaF ₂ type – predicted	–645.9433	–643.8379
SrSi ₂ -like type – predicted	–645.8936	–643.7880

Next, we consider the TiSi₂ type modification, which is an energetically favorable structure candidate, with a similar energy as the experimentally observed modifications of WSi_2 (see Table 3). Although, the TiSi₂ type modification of WSi_2 appears to be metastable, its $E(V)$ curve is very close to the one computed for the experimentally found low temperature CrSi₂ modification, and the TiSi₂ type is an even better structure candidate at expanded volumes than the CrSi₂ type and possibly also than the MoSi₂ type (see Figure 5). This could be an indication of a possible synthesis route for the TiSi₂ type as a novel WSi_2 modification: perhaps the actual TiSi₂ compound can be used as a template for the deposition of a

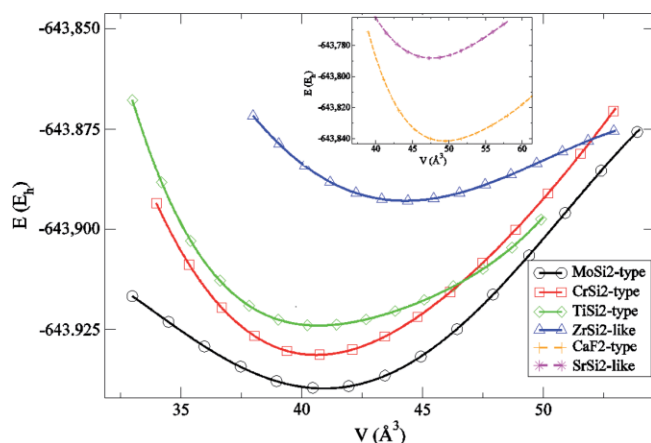


Figure 5. Energy vs. volume curves, $E(V)$, calculated for the investigated structure types in the WSi_2 system, using the LDA functional. The main Figure shows the $E(V)$ curves for the four most relevant structure types ($MoSi_2$, $CrSi_2$, $TiSi_2$, and $ZrSi_2$ -like), while those of the $SrSi_2$ -like modification and the CaF_2 -type have been placed into an inset because of their very high energies compared with the other four structure types. Energies per formula unit are given in hartree (E_h).

W/Si vapor producing an amorphous WSi_x film from which the predicted $TiSi_2$ phase of WSi_2 can be generated by tempering at low temperatures – a type of procedure successfully employed in the past to synthesize metastable compounds.^[64,65]

Another interesting metastable structure candidate in the effective negative pressure region is the $ZrSi_2$ -like modification (Figure 5). However, the $ZrSi_2$ -like modification is energetically considerably less favorable than the $CrSi_2$ and the $TiSi_2$ phases. Nevertheless, Figure 5 indicates that at large effective negative pressures it is likely to become the thermodynamically stable phase, and thus a similar synthesis approach as the one suggested above for the $TiSi_2$ -type phase may be feasible. On the other hand, the other predicted structures with $SrSi_2$ -like and CaF_2 type structures show much higher total energies (see Table 3 and Figure 5), and these modifications would probably be very difficult to synthesize in the WSi_2 system.

We therefore conclude that our data-mining study has generated a variety of structure candidates some of which appear to be promising candidates for an alternative new WSi_2 modification, and further investigations of their structural, physical and chemical properties are planned.

4 Conclusions

The W-Si system is one of the most important refractory metal–silicon systems due to their great technological and industrial applications. In order to investigate tungsten based silicide, we have performed combined experimental and theoretical investigations. Tungsten disilicide (WSi_2) was synthesized by simple thermal treatment at 1350 °C for 4 h in an argon atmosphere. We found that optimizing the synthesis conditions led to a mix of pure WSi_2 (85 %) and W_5Si_3 (15 %) phases, with negligible amounts of impurity phases present.

Finally, new structures have been suggested for WSi_2 and investigated using first-principles calculations within the density-functional theory (DFT) approximation. The LDA and PBE based calculations show excellent agreement with experimental observations and previous calculations (where available). In addition, we discuss several not-yet observed or computationally studied modifications of tungsten disilicide, which might be accessible experimentally. A successful synthesis of these new WSi_2 phases would have a great impact on the scientific, technological and industrial application of tungsten based silicides

Acknowledgements

This work has been supported by the grant No. 45012 and No. 171001 from the Ministry of Education, Science and Technological Development of the Republic of Serbia. The authors thank *M. Rosic*, *K. Djuris*, *B. Babic*, and *V. Maksimovic* for valuable discussions. The authors thank *Prof. R. Dovesi*, *Prof. K. Doll*, and Crystal Solutions for software support.

Keywords: Tungsten disilicide; Tungsten; XRPD analysis

References

- [1] S. Oyama, *Introduction to the Chemistry of Transition Metal Carbides and Nitrides*, in *The Chemistry of Transition Metal Carbides and Nitrides*, Springer Netherlands, **1996**, pp. 1–27.
- [2] H. O. Pierson, *Handbook of Refractory Carbides and Nitrides: Properties, Characteristics, Processing and Applications*, Elsevier Inc., **1996**.
- [3] C. Gelain, A. Cassuto, P. Le Goff, *Oxidation Met.* **1971**, *3*, 153.
- [4] S. L. Kharatyan, H. Chatilyan, A. B. Harutyunyan, *Defect Diffusion Forum* **2001**, *194–199*, 1557.
- [5] K. H. Lee, J. K. Yoon, J. K. Lee, J. M. Doh, K. T. Hong, W. Y. Yoon, *Surface Coatings Technol.* **2004**, *187*, 146.
- [6] J. K. Yoon, K. W. Lee, S. J. Chung, I. J. Shon, J. M. Doh, G. H. Kim, *J. Alloys Compd.* **2006**, *420*, 199.
- [7] L. X. Cai, H. M. Wang, *Appl. Surf. Sci.* **2004**, *235*, 501.
- [8] J. Y. Suh, S. E. Shin, D. H. Bae, *Powder Technol.* **2015**, *289*, 401.
- [9] J. Luković, B. Babić, D. Bučevac, M. Prekajski, J. Pantić, Z. Baščarević, B. Matović, *Ceram. Int.* **2015**, *41*, 1271.
- [10] F. Mohammadi, K. C. Saraswat, *J. Electrochem. Soc.* **1980**, *127*, 450.
- [11] M. Y. Tsai, C. S. Petersson, F. M. d'Heurle, V. Maniscalco, *Appl. Phys. Lett.* **1980**, *37*, 295.
- [12] D. L. Kwong, D. C. Meyers, *Appl. Phys. Lett.* **1985**, *47*, 688.
- [13] B. Y. Tsaur, C. K. Chen, C. H. Anderson Jr., D. L. Kwong, *J. Appl. Phys.* **1998**, *57*, 1890.
- [14] K. C. Saraswat, D. L. Brors, J. A. Fair, K. A. Monnig, R. Beyers, *IEEE Trans. Electron Devices* **1983**, *30*, 1497.
- [15] J. M. Jasinski, B. S. Meyerson, B. A. Scott, *Low Pressure Chemical Vapor Deposition of Tungsten Silicide*, U. S. Patent Nr. US 4684542 A, International Business Machines Corporation, United States, **1987**.
- [16] M. Y. Tsai, F. M. d'Heurle, C. S. Petersson, R. W. Johnson, *J. Appl. Phys.* **1981**, *52*, 5350.
- [17] Y. Shioya, T. Itoh, I. Kobayashi, M. Maeda, *J. Electrochem. Soc.* **1986**, *133*, 1475.
- [18] H. S. Kim, J. K. Yoon, G. H. Kim, J. M. Doh, S. I. Kwun, K. T. Hong, *Intermetallics* **2008**, *16*, 360.
- [19] H. Kudielka, H. Nowotny, *Monatsh. Chem.* **1956**, *87*, 471.
- [20] A. N. Christensen, *J. Cryst. Growth* **1993**, *129*, 266.

- [21] Y. Harada, M. Morinaga, D. Saso, M. Takata, M. Sakata, *Intermetallics* **1998**, *6*, 523.
- [22] F. M. d'Heurle, C. S. Petersson, M. Y. Tsai, *J. Appl. Phys.* **1980**, *51*, 5976.
- [23] M. Y. Tsai, F. M. d'Heurle, C. S. Petersson, R. W. Johnson, *J. Appl. Phys.* **1981**, *52*, 5350.
- [24] J. H. Liang, D. S. Chao, *Surface Coatings Technol.* **2001**, *140*, 116.
- [25] J. Stoetzel, T. Schneider, M. M. Mueller, H.-J. Kleebe, H. Wiggers, G. Schierning, R. Schmechel, *Acta Materialia* **2017**, *125*, 321.
- [26] J. Rodriguez-Carvajal, Collected Abstract of Powder Diffraction Meeting, Toulouse, France **1990**, p. 127.
- [27] R. Dovesi, V. R. Saunders, C. Roetti, R. Orlando, C. M. Zicovich-Wilson, F. Pascale, B. Civalleri, K. Doll, N. M. Harrison, I. J. Bush, P. D'Arco, M. Llunell, *CRYSTAL14 User's Manual*, University of Torino, Torino, Italy **2009**.
- [28] R. Dovesi, R. Orlando, B. Civalleri, C. Roetti, V. R. Saunders, C. M. Zicovich-Wilson, *Z. Kristallogr.* **2005**, *220*, 571.
- [29] F. Pascale, C. M. Zicovich-Wilson, R. Orlando, C. Roetti, P. Ugliengo, R. Dovesi, *J. Phys. Chem. B* **2005**, *109*, 6146.
- [30] D. Andrae, U. Haeussermann, M. Dolg, H. Stoll, H. Preuss, *Theor. Chim. Acta* **1990**, *77*, 123.
- [31] K. Doll, V. R. Saunders, N. M. Harrison, *Int. J. Quantum Chem.* **2001**, *82*, 1.
- [32] K. Doll, *Mol. Phys.* **2010**, *108*, 223.
- [33] B. Civalleri, P. D'Arco, R. Orlando, V. R. Saunders, R. Dovesi, *Chem. Phys. Lett.* **2001**, *348*, 131.
- [34] J. C. Schön, Z. Cancarevic, M. Jansen, *J. Chem. Phys.* **2004**, *121*, 2289.
- [35] J. C. Schön, I. V. Pentin, M. Jansen, *Phys. Chem. Chem. Phys.* **2006**, *8*, 1778.
- [36] D. Zagorac, K. Doll, J. C. Schön, M. Jansen, *Phys. Rev. B* **2011**, *84*, 045206.
- [37] D. Zagorac, J. C. Schön, J. Zagorac, M. Jansen, *RSC Adv.* **2015**, *5*, 25929.
- [38] J. P. Perdew, A. Zunger, *Phys. Rev. B* **1981**, *23*, 5048.
- [39] J. P. Perdew, K. Burke, M. Ernzerhof, *Phys. Rev. Lett.* **1996**, *77*, 3865.
- [40] R. Hundt, J. C. Schön, A. Hannemann, M. Jansen, *J. Appl. Crystallogr.* **1999**, *32*, 413.
- [41] A. Hannemann, R. Hundt, J. C. Schön, M. Jansen, *J. Appl. Crystallogr.* **1998**, *31*, 922.
- [42] R. Hundt, *KPLOT: A Program for Plotting and Investigation of Crystal Structures*, Technicum Scientific Publishing, Stuttgart, Germany, 2017.
- [43] R. Hundt, J. C. Schön, M. Jansen, *J. Appl. Crystallogr.* **2006**, *39*, 6.
- [44] K. Momma, F. Izumi, *J. Appl. Crystallogr.* **2008**, *41*, 653.
- [45] J. C. Schön, M. Jansen, *Angew. Chem. Int. Ed. Engl.* **1996**, *35*, 1268.
- [46] S. M. Woodley, C. R. A. Catlow, *Nat. Mater.* **2008**, *7*, 937.
- [47] J. C. Schön, K. Doll, M. Jansen, *Phys. Status Solidi B* **2010**, *247*, 23.
- [48] A. R. Oganov (Editor), *Modern Methods of Crystal Structure Prediction*, Wiley VCh, Weinheim, **2011**.
- [49] J. C. Schön, *Z. Anorg. Allg. Chem.* **2014**, *640*, 2717.
- [50] S. Curtarolo, D. Morgan, K. Persson, J. Rodgers, G. Ceder, *Phys. Rev. Lett.* **2003**, *91*, 135503.
- [51] G. Ceder, D. Morgan, C. Fischer, K. Tibbetts, S. Curtarolo, *MRS Bull.* **2006**, *31*, 981.
- [52] J. Zagorac, D. Zagorac, A. Zarubica, J. C. Schön, K. Djuris, B. Matovic, *Acta Crystallogr., Sect. B* **2014**, *70*, 809.
- [53] D. Zagorac, J. C. Schön, M. Jansen, *Proc. Appl. Ceram.* **2013**, *7*, 37.
- [54] M. Čebela, D. Zagorac, K. Batalović, J. Radaković, B. Stojadinović, V. Spasojević, R. Hercigonja, *Ceram. Int.* **2017**, *43*, 1256.
- [55] G. Bergerhoff, I. D. Brown, *Crystallographic Databases* (Ed. F. H. Allen, G. Bergerhoff, R. Sievers), Chester, International Union of Crystallography, **1987**.
- [56] *Pearson's Handbook of Crystallographic Data for Intermetallic Phases* (Eds.: P. Villars, L. D. Calvert), 2nd ed., Materials Park (OH), ASM International; **1991**.
- [57] G. Shao, *Acta Materialia* **2005**, *53*, 3729.
- [58] W. Jeitschko, *Acta Crystallogr., Sect. B* **1977**, *33*, 2347.
- [59] H. Nowotny, in: *Electronic Structure and Alloy Chemistry of the Transition Elements* (Ed.: P. A. Beck), Interscience, New York, **1963**, pp. 179–220.
- [60] L. F. Mattheiss, *Phys. Rev. B* **1992**, *45*, 3252.
- [61] G. E. Pringle, *Acta Crystallogr., Sect. B* **1972**, *28*, 2326.
- [62] D. N. Batchelder, R. O. Simmons, *J. Chem. Phys.* **1964**, *41*, 2324.
- [63] K. C. Bhamu, J. Sahariya, B. L. Ahuja, *J. Phys. Chem. Solids* **2013**, *74*, 765.
- [64] D. C. Johnson, *Curr. Opin. Solid State Mater. Sci.* **1998**, *3*, 159.
- [65] D. Fischer, M. Jansen, *Angew. Chem. Int. Ed.* **2002**, *41*, 1755.

Received: August 31, 2017

Published online: November 23, 2017